Bit Error Rate Reduction by Smart UWB Antenna Array in Indoor Wireless Communication

doi:10.6180/jase.2012.15.2.07

淡江理工學刊, 15(2), 2012

Journal of Applied Science and Engineering, 15(2), 2012

作者/Author： Chien-Ching Chiu;Chien-Hung Chen;Shu-Han Liao;Kuan-Chung Chen

頁數/Page： 139-148

出版日期/Publication Date：2012/06

Bit Error Rate Reduction by Smart UWB Antenna Array in Indoor Wireless Communication

Chien-Ching Chiu[1]*, Chien-Hung Chen[2], Shu-Han Liao[1] and Kuan-Chung Chen[1]

[1]*Department of Electrical Engineering, Tamkang University, Tamsui, Taiwan 251, R.O.C.*
[2]*Department of Computer and Communication Engineering, Taipei College of Maritime Technology, Taipei, Taiwan 111, R.O.C.*

Abstract

In this paper, a new ultra wideband circular antenna array (UCAA) combining genetic algorithm to minimize the bit error rate (BER) is proposed. The ultra wideband (UWB) impulse responses of the indoor channel for any transmitter-receiver location are computed by applying shooting and bouncing ray/image (SBR/Image) techniques, inverse fast Fourier transform and Hermitian processing. By using the impulse response of multipath channel, the BER performance of the binary pulse amplitude modulation (B-PAM) impulse radio (IR) UWB system with circular antenna array can be calculated. Based on the topography of the antenna and the BER formula, the array pattern synthesis problem can be reformulated into an optimization problem and solved by the genetic algorithm. Our approach is not only choosing BER as the object function instead of sidelobe level of the antenna pattern, but also considering the antenna feed length effect of each array element. The strong point of the genetic algorithm is that it can find out the solution even if the performance index cannot be formulated by simple equations. Simulation results show that the synthesized antenna array pattern is effective to focus maximum gain to the LOS path which scales as the number of array elements. In other words, the receiver can increase the received signal energy to noise ratio. The synthesized array pattern also can mitigate severe multipath fading in complex propagation environment. As a result, the BER can be reduced substantially in indoor UWB communication system.

***Key Words*:** UWB, Genetic Algorithm, BER, Feed Length, Circular Antenna Array, SBR/Image

1. Introduction

Ultra wideband (UWB) technology is an ideal candidate for a low power, low cost, high data rate, and short range wireless communication system. According to the Federal Communication Commission (FCC), UWB signal is defined as a signal having fractional bandwidth greater than 20% of the center frequency [1]. Ultra wide bandwidth of the system causes antenna design to be a new challenge [2–5]. This is because the multipath fading and interferences become more apparent than in narrow band system. In order to overcome this phenomenon, smart antenna technology is envisaged as one of possible solutions.

Smart antennas employ arrays of antenna elements and can integrate multiple antenna elements with a signal processing. These smart antennas combine the signals from multiple antennas in a way that mitigates multipath fading and maximizes the output signal-to-noise ratio. It can dramatically increase the performance of a communication system. The smart antenna technology in wireless communication can apply to the receiver [6,7] and the transmitter [8,9]. The smart antenna technique at receiver is to perform combining or choosing in

*Corresponding author. E-mail: chiu@ee.tku.edu.tw

order to improve the quality of the received signal. When using the smart antenna to be a transmitter, it can focus the synthesized antenna array pattern to optimize available processing gain to the receiver by adjusting the excitation phase delay and amplitude of each antenna array element and so on.

In the past, most papers apply genetic algorithms for searching the minimum sidelobe level of the antenna [10]. However, this pattern cannot guarantee to obtain the minimum BER performance. In this paper, we propose a smart ultra wideband circular antenna array at the transmitter to synthesize an array pattern for minimizing the BER performance in a UWB communication system. Unlike in a narrow band communication system, the UWB communication system spans a wide bandwidth in the frequency domain. In fact, adjusting the same excitation phase delay of the UWB antenna for different frequencies is difficulty. Thus we control the feed length of the array element. It provides the excitation phase delay which varies with different frequencies to synthesize the antenna array pattern.

When synthesizing the antenna array pattern to minimize the BER, the excitation problem is reformulated as an optimization problem and the constraint conditions are often highly nonlinear and non-differentiable. Thus, we use the genetic algorithm to regulate the antenna feed length of each array element to minimize the BER performance. As a result, the receiver can increase the received signal energy to noise ratio. Moreover, it can mitigate severe multipath fading and reduce the effective delay spread of the channel.

In this paper, the genetic algorithm is used to regulate the antenna feed length of each array element to minimize the BER performance of the communication system. The remaining sections of this paper are organized as follows: section 2 briefly explains the formulation of the problem which includes antenna pattern, channel modeling and the BER calculation. Section 3 describes the genetic algorithm. The propagation modeling and numerical results are then presented in section 4 and conclusion is made in section 5.

2. System Description

The entire link can be described in terms of the block diagram in Figure 1. It shows the B-PAM UWB modulator, equivalent baseband impulse response $h_b(t)$ which includes the effect of the circular antenna array, a correlation receiver and feed length controller (regulated by the Genetic algorithm to minimize BER).

2.1 Circular Array Pattern

We consider a circular array of N UWB printed dipole antenna, as shown in Figure 2. Each element is apart along a circle of radius Γ (= 5 cm) which is corresponding to the half wavelength of 3 GHz. Each element, as shown in Figure 3, is the UWB printed dipole antenna with circular arms, which has been designed in [11,12].

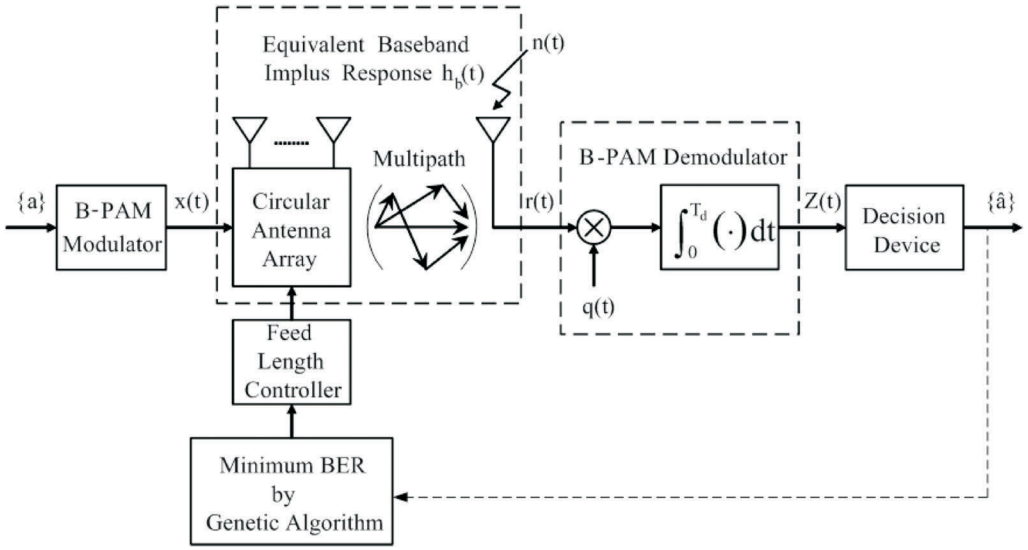

Figure 1. Block diagram of the simulated system.

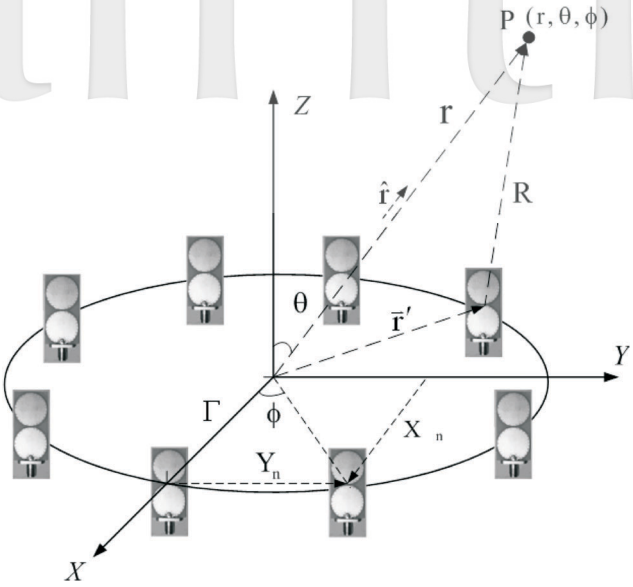

Figure 2. Geometry of a circular antenna of 8 UWB printed dipole antennas.

The overall dimensions of the structure are 40.5 mm × 20.5 mm × 1 mm, with an arm diameter of 19.5 mm. The input impedance bandwidth is from 3 GHz up to more than 11 GHz. The radiation pattern between 3 GHz and 6 GHz is omnidirectional in the azimuth plane, which is interesting for communications between objects having undefined position in relation to each other. Because to this advantage, we use this kind of antenna for circular array element. The array factor of this circular antenna array can be written as

$$AF(\theta,\phi,f)=\sum_{n=1}^{N_T}F_n\exp[-j(k\cdot X_n\sin\theta\cos\phi + k\cdot Y_n\sin\theta\sin\phi+\psi_n)] \quad (1)$$

where θ and ϕ are the spherical coordinate angles from the origin to the viewpoint in the elevation plane and azimuth plane. F is the frequency of a sinusoidal wave. N_T is the element number. $k = 2\pi/\lambda$ is the wavenumber, where λ is the wavelength of the sinusoidal wave. ψ_n is the excitation current phase delay of the n-th element and F_n is the element excitation current amplitude of the n-th element. In this paper, all F_n are set to 1. X_n and Y_n are the positions of the n-th array element. Thus the total radiation vector can be expressed as

$$\vec{N}(\theta,\phi,f)=AF(\theta,\phi,f)\cdot\vec{N}_e(\theta,\phi,f) \quad (2)$$

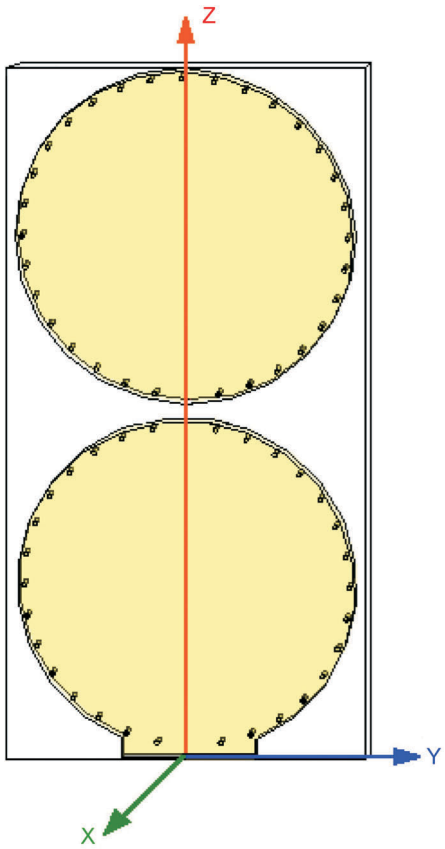

Figure 3. A UWB printed dipole antenna with circular arms.

where $\vec{N}(\theta,\phi,f)$ is the radiation vector of individual element which can be obtained by the HFSS software based on the finite element method.

2.2 UWB Channel Modeling

Because the UWB communication spans a wide bandwidth in the frequency domain, the channel impulse response variations are significant for different types of antennas [13,14]. As a result, we do not only describe the antenna radiation pattern which varies with different frequencies but also use the SBR/Image technique to calculate the channel impulse response which includes angular characteristics of radiation patterns and the variation between different frequencies of wave propagation.

SBR/Image [15–23] techniques are good techniques to calculate channel frequency response for wireless communication [24,25]. In this paper, we develop SBR/Image techniques including the antenna pattern to model our simulation channel. It can perform the identification of major scattering objects causing reflection, diffraction and penetration in our simulation environment. The

SBR/Image technique conceptually assumes that many triangular ray tubes (not rays) are shot from a transmitter. Here, the triangular ray tubes whose vertexes are on a sphere are determined by the following method. First, we construct an icosahedron which is made of 20 identical equilateral triangles. Then, each triangle of the icosahedron is tessellated into a lot of smaller equilateral triangles. Finally, these small triangles are projected on to the sphere and each ray tube whose vertexes are determined by the small equilateral triangle is constructed. Then, each ray tube will bounce and penetrate in the simulate environments. If the receiver falls within the reflected ray tube, the contribution of the ray tube to the receiver can be attributed to an equivalent source (image). Using these images and received fields, the channel frequency response can be obtained as following

$$H(f) = \sum_{i=1}^{N_T} \left| a_i(f) \right| e^{j\theta_i(f)} \tag{3}$$

where f is the frequency of the sinusoidal wave, i is the path index, θ_i is the i-th phase shift, $\left|a_i\right|$ is the i-th receiving magnitude which depends on the radiation vector of the transmitting and receiving antenna in (2). Note that the receiving antenna in our simulation is only one omnidirectional UWB dipole antenna and the transmitter is the UWB circular antenna array (UCAA) which has been described in above section. The channel frequency response of UWB can be calculated form equation (3) in the frequency range of UWB.

The frequency response is transformed to the time domain by using the inverse Fast Fourier Transform with the Hermitian signal processing [26]. Therefore, the time domain impulse response of the equivalent baseband can be written as follows

$$h_b(t) = \sum_{m=1}^{M_T} \alpha_m \delta(t - \tau_m) \tag{4}$$

where M_T is the number of paths. α_m and τ_m are the channel gain and time delay for the m-th path, respectively.

2.3 Formulation of BER

As shown in Figure 1, {a} is the input binary data stream and {â} is the output binary data stream after demodulator and decision device. When {a} passing through the B-PAM modulator, the transmitted UWB pulse stream is expressed as follows:

$$x(t) = \sum_{n=0}^{\infty} p(t - nT_d) d_n \tag{5}$$

where E_t is the average transmitted energy and $p(t)$ is the transmitted waveform. $d_n \in \{\pm 1\}$ is a B-PAM symbol and is assumed to be independent identically distributed (i.i.d.). T_d is the duration of the transmitting signal. The transmitted waveform $p(t)$ is the Gaussian waveform with ultra-short duration T_p at the nanosecond scale. Note that T_d is the duration of the transmitting signal and T_p is the pulse duration. The value of T_d is usually much larger than that of T_p. The Gaussian waveform $p(t)$ can be described by the following expression:

$$p(t) = \frac{1}{\sqrt{2\pi}\sigma} e^{2\frac{-t^2}{\sigma^2}} \tag{6}$$

where t and σ are time and standard deviation of the Gaussian wave, respectively. The average transmit energy symbol E_t can be expressed as

$$E_t = \int_0^{T_d} P^2(t) dt \tag{7}$$

The received signal $r(t)$ can be expressed as follows:

$$r(t) = [x(t) \otimes h_b(t)] + n(t) \tag{8}$$

where $x(t)$ is the transmitted signal and $h_b(t)$ is the impulse response of the equivalent baseband, $n(t)$ is the white Gaussian noise with zero mean and variance $N_0/2$. The correlation receiver samples the received signal at the symbol rate and correlates them with suitably delayed references given by

$$q(t) = p[t - \tau_1 - (n-1)T_d] \tag{9}$$

where τ_1 is the delay time of the first wave. The output of the correlator is [27,28]:

$$\begin{aligned} Z(n) = & \int_{(n-1)T_d}^{nT_d} \left\{ [\sum_{i=0}^{\infty} p(t - iT_d) d_i] \otimes h_b(t) \right\} \cdot q(t) dt \\ & + \int_{(n-1)T_d}^{nT_d} n(t) q(t) dt = V(n) + \eta(n) \end{aligned} \tag{10}$$

It can be shown that the noise components $\eta(t)$ of (10) are uncorrelated Gaussian random variables with zero mean. The variance of the output noise η is

$$\sigma^2 = \frac{N_0}{2} E_t \tag{11}$$

The conditional error probability of the n-th bit is thus expressed by:

$$P_e\left[Z(n) \mid \vec{d}\right] = \frac{1}{2} erfc\left[\frac{V(n)}{\sqrt{2}\sigma} \cdot (d_n)\right] \tag{12}$$

where $erfc(x) = \frac{2}{\sqrt{\pi}} \int_x^{\infty} e^{-y^2} dy$ is the complementary error function and $\{\vec{d}\} = \{d_0, d_1, \ldots d_n\}$ is the binary sequence. Finally, the average BER for B-PAM IR UWB system can be expressed as [29]

$$BER = \sum_{i=1}^{2^n} P(\vec{d}) \cdot \frac{1}{2} erfc\left[\frac{V(i)}{\sqrt{2}\sigma} \cdot (d_n)\right] \tag{13}$$

3. Genetic Algorithm

Genetic algorithms are global numerical optimization methods based on genetic recombination and evaluation in nature [30,31]. They use the iterative optimization procedures, which start with a randomly selected population of potential solutions. Then, iterative optimization procedures gradually evolve toward a better solution through the application of the genetic operators. Genetic algorithms typically operate on a discretized and encoded representation of the parameters rather than on the parameters themselves. These representations are often considered to be "chromosomes", while the individual element, which constitutes chromosomes, is the "gene". Simple but often very effective chromosome representations for optimization problem involving several continuous parameters can be obtained through the juxtaposition of discretized binary representations of the individual parameter.

When analyzing the circular antenna array, the feed length of each array element provides the phase delay of excitation current which varies with different frequencies. The relationship between the n-th antenna feed length ℓ_n and the excitation current phase delay ψ_n can be expressed as follows:

$$\psi_n = \frac{2\pi}{\lambda} \ell_n \tag{14}$$

where λ is the wavelength. Thus, we regulate the antenna feed length of each array element to get a optimal radiation pattern which can minimize the BER performance. The feed length of each array element can be decoded by the following equation:

$$\ell_n = Q_{\min} + \frac{Q_{\max} - Q_{\min}}{2^M - 1} \sum_{i=0}^{M-1} b_i^{\ell_n} 2^i \tag{15}$$

where $b_0^{\ell_n}, b_1^{\ell_n}, \ldots, b_{M-1}^{\ell_n}$ (genes) are M-bit strings of the binary representation of ℓ_n.The $Q_{\min}$ and $Q_{\max}$ are the minimum and the maximum values admissible for ℓ_n, respectively. In practical cases, $Q_{\min}$ and $Q_{\max}$ can be determined by the prior knowledge of the objects. Therefore, we set the $Q_{\min} = 0.0$ cm and $Q_{\max} = 10.0$ cm which is according to the minimum frequency 3 GHz. Then the unknown coefficients in (15) are described by a $N_T \times M$ bit string (chromosome). The genetic algorithm starts with a population containing a total of N_p candidates (i.e., N_p is the population size). Each candidate is described by a chromosome. Then the initial population can simply be created by taking N_p random chromosomes. GA iteratively generates a new population, which is derived from the previous population through the application of the reproduction, crossover, and mutation operators.

The genetic algorithm is used to maximize the following fitness function (FF):

$$FF = \left\{\sum_{i=1}^{2^n} P(\vec{d}) \cdot \frac{1}{2} erfc\left[\frac{V(i)}{\sqrt{2}\sigma} \cdot (d_n)\right]\right\}^{-1} \tag{16}$$

where FF is the inverse of the average BER for B-PAM IR UWB system. Through repeated applications of reproduction, crossover, and mutation operators, the initial population is transformed into a new population in an iterative manner. New populations will contain increasingly better chromosomes and will eventually converge to an optimal population that consists of the optimal chromosomes. In our simulation, when the fit-

ness function is bigger than the threshold value or GA does not find a better individual within 300 successive generations, the genetic algorithm will be terminated and a solution is then obtained.

4. Numerical Results

A realistic environment is investigated. It consists of a living room with dimensions 10 m × 10 m × 3 m, housing one metallic cupboard and three wooden bookcases. Both of the cupboard and bookcase are 2 meter in height. The radio wave can penetrate through the wooden bookcase and is totally reflected by the metallic cupboard. The plan view of the simulated environment is shown in Figure 4. Tx and Rx1, Rx2 antennas were all mounted 1 meter above the floor. The transmitter Tx position is (7 m, 5 m, 1 m). We simulated two scenarios with different Rx positions. Scenario I has a line-of-sight path to the Rx1 (3 m, 8.5 m, 1 m). Tx and Rx1 are at a distance of approximately 5 meter. Scenario II has no line-of-sight path to the Rx2 (5 m, 1 m, 1 m), since the wooden bookcase was higher than the Tx and Rx2. The Tx - Rx2 distance on the horizontal plane is 4.3 meter in Scenarios II. A three-dimensional SBR/Image technique combined antenna radiation pattern has been presented in this paper. This technique is used to calculate the UWB channel impulse response for each location of the receiver.

Based on the channel impulse response, the number of multipath components, the RMS delay spread τ_{RMS} and the Mean Excess Delay τ_{MED} are computed. Furthermore, we use the impulse response to calculate the BER.

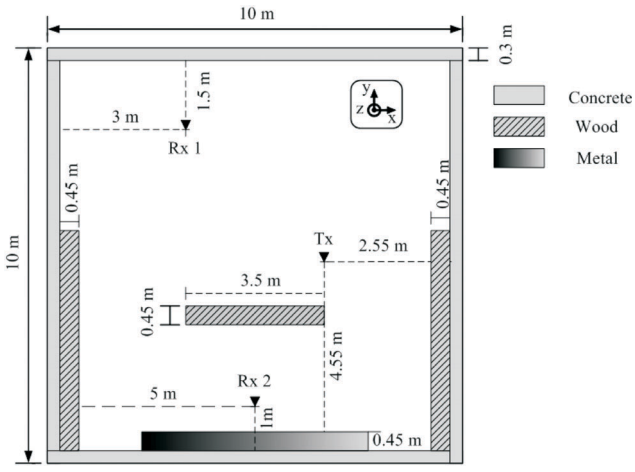

Figure 4. A plan view of the simulated environment.

The frequency range for the UWB channel is simulated from 3 GHz to 6 GHz, because the array element has the omnidirectional characteristic in this frequency range [11]. Other simulation specifications are summarized in Table 1.

Figure 5 (a), shows the channel impulse response for Scenario I using three kinds of transmitting antennas: (a) Only one UWB printed dipole antenna (OUA) (b) A circular array of eight UWB printed Dipole antenna, each element antenna has the same feed Length without GA regulating (NOGA-UCAA) (c) A circular array of eight UWB printed dipole antenna , each element antenna feed length was regulated by GA(GA-UCAA). In Figure 5, all the first peak is received around 16ns which is correlated with 5 meter distance from the direct LOS path. The number of resolved multipath components in Figure 5(a) is greater than the number in Figure 5(c), since the directive radiation pattern in GA-UCAA provides focusing gain to the LOS and mitigates the multipath. The energy seems to be spread over less paths than for the omnidirectional transmitter (OUA). In Figure 5(b), the radiation pattern of the circular antenna array also has directive characteristic. However, it can not provide the largest synthetic gain to the LOS path. In other words, it has different gains in each direction including LOS and NLOS path. As a result, the multipath phenomenon in Figure 5(b) is worse than the phenomenon in Figure 5(c). Comparing the first peak value in Figures 5(a) and (c), it is found that the peak value in Figure 5(c) is N times as that in Figure 5(a). Here N is the number of array elements.

In order to determine the multipath effect, the τ_{RMS} and τ_{MED} were calculated. A summary of these values are given in Table 2 for Scenarios I and II, respectively,

Table 1. Specifications of the antenna and genetic algorithm

Antenna	UWB circular antenna array
Number of array element (N)	8
Circle of radius Γ	6.75 (cm)
Polarization of Tx-Rx	Vertical-Vertical
Transmitted signal to noise ratio	At least 20 dB
GA population size	200
Binary string length	10
Search range of the feed length	0.0 to 10.0 (cm)
The probability of crossover and mutation	0.5 and 0.02

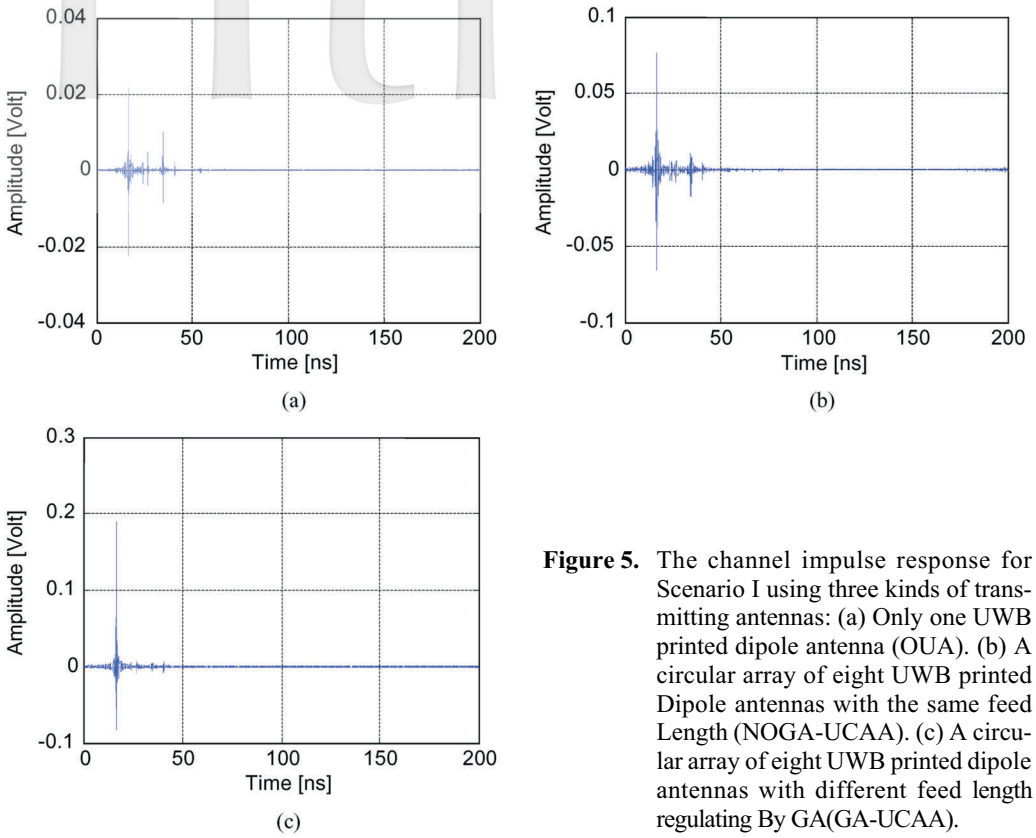

Figure 5. The channel impulse response for Scenario I using three kinds of transmitting antennas: (a) Only one UWB printed dipole antenna (OUA). (b) A circular array of eight UWB printed Dipole antennas with the same feed Length (NOGA-UCAA). (c) A circular array of eight UWB printed dipole antennas with different feed length regulating By GA(GA-UCAA).

Table 2. Mean excess delay and RMS delay spread for the two Scenarios

Transmitting Antennas / Scenarios	OUA		NOGA-UCAA		GA-UCAA	
	τ_{MED} (ns)	τ_{RMS} (ns)	τ_{MED} (ns)	τ_{RMS} (ns)	τ_{MED} (ns)	τ_{RMS} (ns)
Scenario I	3.53	7.38	3.43	8.01	0.51	3.52
Scenario II	11.88	12.55	11.08	12.04	10.91	6.72

which clearly shows the τ_{MED} increase for the NLOS case (Scenario II). For the LOS case in Scenario I, the τ_{RMS} in OUA and in GA-UCAA is 7.38 ns and 3.52 ns respectively. It is clear that τ_{RMS} for the GA-UCAA case is the smallest, since the directive antenna can mitigate multipath effect. Figure 6 shows the BER V.S. SNR for Scenario I using three kinds of transmitters. Here SNR is defined as the ratio of the average transmitting power to the noise power. The results show that the BER curve decreases greatly when the GA-UCAA is used as transmitter. It is due to the fact that the GA-UCAA can minimize the fading and reduce the mulitpath effects. It also can focus the synthesized antenna array pattern to optimize the available processing gain to the receiver.

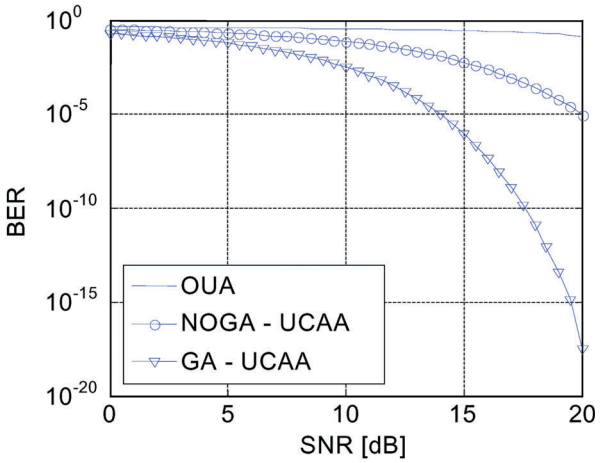

Figure 6. BER vs. SNR over Scenario I for three kinds of transmitter.

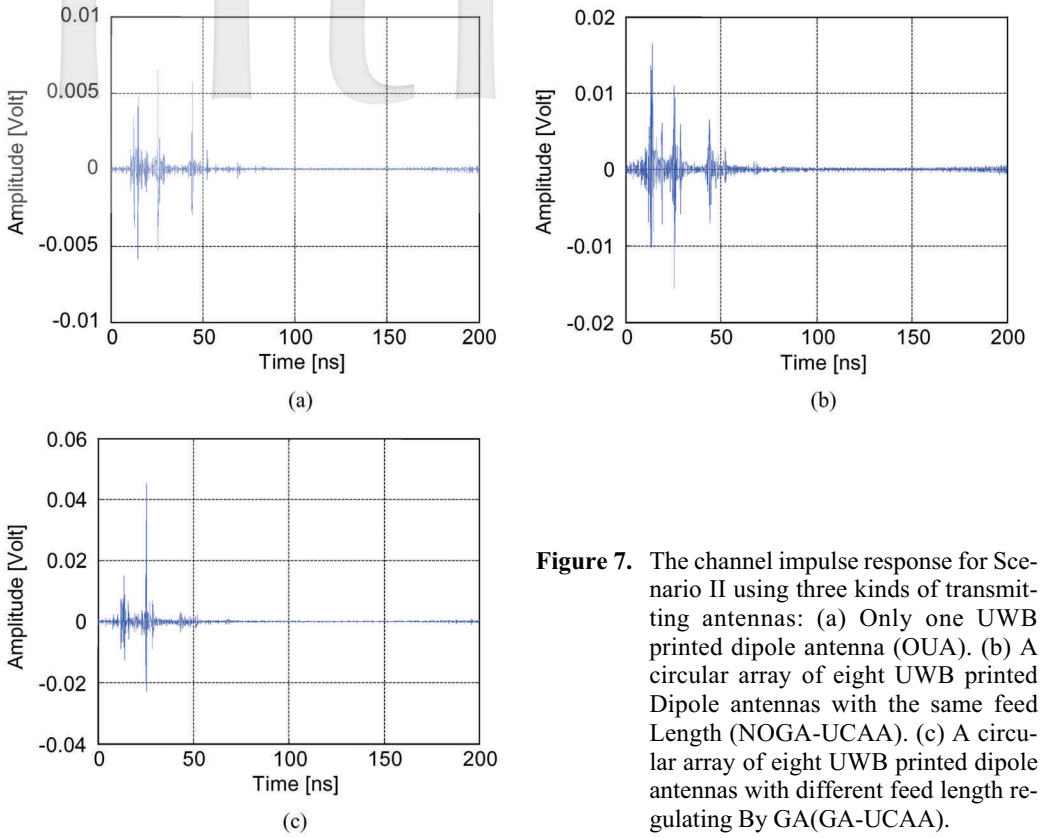

Figure 7. The channel impulse response for Scenario II using three kinds of transmitting antennas: (a) Only one UWB printed dipole antenna (OUA). (b) A circular array of eight UWB printed Dipole antennas with the same feed Length (NOGA-UCAA). (c) A circular array of eight UWB printed dipole antennas with different feed length regulating By GA(GA-UCAA).

Figure 7 shows the channel impulse response for Scenario II using three kinds of transmitters. In this scenario, we consider a situation which has no LOS path of all the three channels. The multipath phenomenon in Figure 7(b) is the worst. It was noted that the radiation pattern of the circular antenna array different gains in each direction. The energy seems to be spread over more paths than that for the omnidirectional transmitter in Figure 7(a). In Figure 7(c), it is clear that the maximum peak value is up to 0.045V which is the highest peak value of the three kinds of transmitters. It also shows the number of multipath components has been clearly reduced. It is due to the fact that the GA-UCAA can focus the synthesized antenna array pattern to optimize the available processing gain to the receiver.

Table 2 also shows the RMS delay spread τ_{RMS} decrease when using the GA-UCAA to be the transmitting antenna in the Scenario II. Figure 8 shows the BER vs. SNR for Scenario II using three kinds of transmitters. The results show that the BER curve decrease when using the GA-UCAA to be transmitter.

Tables 3 and 4 show optimized feed lengths and excitation current amplitudes for each antenna element in the Scenario I and Scenario II, respectively.

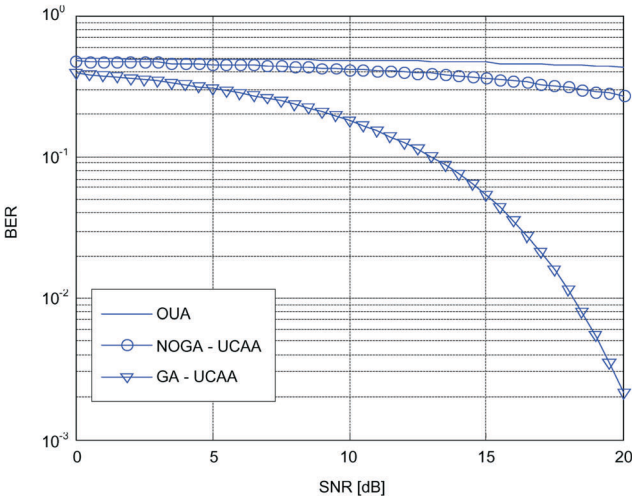

Figure 8. BER vs. SNR over Scenario II for three kinds of transmitter.

All of the above results demonstrate the GA-UCAA which is presented in this paper is powerful. When applying this antenna array to LOS and NLOS propagation environment, it can increase the ratio of combined receiving signal energy to noise. It also can mitigate severe multipath fading in complex propagation environment.

Table 3. Optimized feed lengths and excitation current amplitudes for each antenna element (Scenario I)

n-th element	feed length (cm)	excitation current amplitude (volt)
1	5.034213	0.999
2	5.816227	0.999
3	3.782991	0.999
4	4.731183	0.999
5	0.4105572	0.999
6	1.818182	0.999
7	1.290323	0.999
8	0.3812317	0.999

Table 4. Optimized feed lengths and excitation current amplitudes for each antenna element (Scenario II)

n-th element	feed length (cm)	excitation current amplitude (volt)
1	7.869013	0.999
2	9.990225	0.999
3	5.014663	0.999
4	2.629521	0.999
5	3.059628	0.999
6	7.272727	0.999
7	6.129032	0.999
8	8.602151	0.999

For these reasons, the BER can be reduced substantially in indoor UWB communication system.

5. Conclusion

Using the smart UWB circular antenna array to minimize the BER performance in indoor wireless local loop is presented. The impulse response of the channel is computed by SBR/Image techniques, inverse fast Fourier transform and Hermitian processing. By using the impulse response of the multipath channel and the genetic algorithm synthesizing optimal antenna radiation pattern, the BER performance of a B-PAM IR UWB communication system is investigated. Based on the BER formulation, the synthesis problem can be reformulated into an optimization problem. In this paper, the fitness function is defined as the reciprocal of BER of the system. The genetic algorithm maximizes the fitness function by adjust the feed length of each antenna. Numerical results show that the BER can be reduced substantially in indoor UWB communication system.

Acknowledgment

This work was supported by National to Science Council, Republic of China, under Grant NSC-96-2221-E-229-001.

References

[1] Federal Communications Commission, "Revision of Part 15 of the Commission's Rules Regarding Ultra-Wideband Transmission System, FIRST REPORT AND ORDER," *FCC, ET Docket*, pp. 1–118 (2002).

[2] Colak, S., Wong, T. F. and Serbest, A. H., "UWB Dipole Array with Equally Spaced Elements of Different Lengths," *2007 IEEE International Conference on Ultra-Wideband*, pp. 789–793 (2007).

[3] Malik, W. Q., Edwards, D. J. and Stevens, C. J., "Angular-Spectral Antenna Effects in Ultra-Wideband Communications Links," *IEE Proc.-Commun*., Vol. 153 (2006).

[4] Funk, E. E. and Lee, C. H., "Free-Space Power Combining and Beam Steering of Ultra-Wideband Radiation Using an Array of Laser-Triggered Antennas," *IEEE Trans. Microwave Theory Tech*., Vol. 44, pp. 2039–2044 (1996).

[5] Yazdandoost, K. Y. and Kohno, R., "Free-Space Power Combining and Beam Steering of Ultra-Wideband Radiation Using an Array of Laser-Triggered Antennas," *IEEE Communication Magazine*, Vol. 42, pp. 29–32 (2004).

[6] Ghavami, M., "Wideband Smart Antenna Theory Using Rectangular Array Structures," *IEEE Trans. Signal Processing*, Vol. 50, pp. 2143–2151 (2002).

[7] Tarokh, V., Seshadri, N. and Calderbank, A. R., "Space-Time Codes for High Data Rate Wireless Communications: Performance Criterion and Code Construction," *IEEE Trans. Inform. Theory*, Vol. 44, pp. 744–745 (1998).

[8] Chen, C. H. and Chiu, C. C., "Novel Optimum Radiation Pattern by Genetic Algorithms in Indoor Wireless Local Loop," *IST Mobile Summit 2000*, Galway, Ireland (2000). (Proc., pp. 391–399).

[9] Peng, M. and Wang, W., "Comparison of Capacity between Adaptive Tracking and Switched Beam Smart Antenna Techniques in TDD-CDMA Systems," *Microwave, Antenna, Propagation and EMC Technologies for Wireless Communications, 2005*, Vol. 1, pp. 135–139 (2005).

[10] Ares, F. J., Rodriguez, A., Villanueva, E. and Rengarajan, S. R., "Genetic Algorithms in the Design and Optimization of Antenna Array Patterns," *IEEE Trans. Antennas and Propagat*., Vol. 47, pp. 506–510 (1999).

[11] Gueguen, E., Thudor, F. and Chambelin, P., "A Low Cost UWB Printed Dipole Antenna with High Performance," *IEEE International Conference on Ultra-Wideband*, pp. 89–92 (2005).

[12] Talom, F. T., Uguen, B., Rudant, L., Keignart, J., Pintos, J.-F. and Chambelin, P., "Evaluation and Characterization of an UWB Antenna in Time and Frequency Domains," *IEEE International Conference on Ultra-Wideband*, pp. 669–673 (2006).

[13] Manteuffel, D., "Radio Link Characterization Using Real Antenna Integration Scenarios for UWB Consumer Electronic Applications," *Ultra Wideband Systems, Technologies and Applications, 2006. The Institution of Engineering and Technology Seminar*, pp. 123–130 (2006).

[14] El-Hadidy, M. and Kaiser, T., "Impact of Ultra Wide-Band Antennas on Communications in a Spatial Cannel," *1st International Cognitive Radio Oriented Wireless Networks and Communications, 2006*, pp. 1–5 (2006).

[15] Liu, C. L., Ho, M. H., Chiu, C. C. and Cheng, C. Y., "A Comparison of UWB Communication Characteristics for Various Corridors," *ACTA International Journal of Modelling and Simulation*, Vol. 30, pp. 172–177 (2010).

[16] Ho, M. H., Liao, S. H. and Chiu, C. C., "A Novel Smart UWB Antenna Array Design by PSO," *Progress in Electromagnetic Research C*, Vol. 15. pp. 103–115, (2010).

[17] Ho, M. H., Liao, S. H. and Chiu, C. C., "UWB Communication Characteristics for Different Distribution of People and Various Materials of Walls," *Tamkang Journal of Science and Engineering*, Vol. 13, pp. 315–326 (2010).

[18] Liao, S. H., Ho, M. H. and Chiu, C. C., "Bit Error Rate Reduction for Multiusers by Smart UWB Antenna Array," *Progress In Electromagnetic Research C*, Vol. 16. pp. 85–98 (2010).

[19] Liao, S. H., Chiu, C. C., Ho, M. H. and Liu, C. L., "Channel Capacity of Multiple-Input Multiple-Output Ultra Wide Band Systems with Single Co-Channel Interference," *International Journal of Communication Systems*, Vol. 23, pp. 1600–1612 (2010).

[20] Liao, S. H., Chen, H. P., Chiu, C. C. and Liu, C. L. "Channel Capacities of Indoor MIMO-UWB Transmission for Different Material Partitions," *Tamkang Journal of Science and Engineering*, Vol. 14, pp. 49–63 (2011).

[21] Chiu, C. C., Kao, Y. T., Liao, S. H. and Huang, Y. F., "'UWB Communication Characteristics for Different Materials and Shapes of the Stairs," *Journal of Communications*, Vol. 6, pp. 628–632 (2011).

[22] Liao, S. H., Ho, M. H., Chiu, C. C. and Lin, C. H. "Optimal Relay Antenna Location in Indoor Environment Using Particle Swarm Optimizer and Genetic Algorithm," *Wireless Personal Communications*, Vol. 62, pp. 599–615 (2012).

[23] Ho, M. H., Chiu, C. C. and Liao, S. H., "Bit Error Rate Reduction for Circular UWB Antenna by DDE," *International Journal of RF and Microwave Computer-Aided Engineering*, Vol. 22, pp. 260–271 (2012).

[24] Malik, W. Q., Edwards, D. J., Zhang, Y. and Brown, A. K., "Three-Dimensional Equalization of Ultrawideband Antenna Distortion," *in Proc. Int. Conf. Electromagn. Adv. Apps. (ICEAA)*, Torino, Italy (2007).

[25] Yao, R., Chen, Z. and Guo, Z., "An Efficient Multipath Channel Model for UWB Home Networking," *Radio and Wireless Conference, 2004 IEEE*, pp. 511–516 (2004).

[26] Oppermann, I., Hamalainen, M. and Iinatti, J., *UWB Theory and Applications*, John Wiley & Sons (2004).

[27] Homier, E. A. and Scholtz, R. A., "Rapid Acquisition of Ultra-Wideband Signals in the Dense Multi-Path Channel," *IEEE Conference on Ultra Wideband Systems and Technologies*, pp. 105–109 (2002).

[28] Gargin, D. J., "A Fast and Reliable Acquisition Scheme for Detecting Ultra Wide-Band Impulse Radio Signals in the Presence of Multi-Path and Multiple Access Interference," *2004 International Workshop on Ultra Wideband Systems*, pp. 106–110 (2004).

[29] Liu, C. L., Chiu, C. C., Liao, S. H. and Chen, Y. S., "Impact of Metallic Furniture on UWB Channel Statistical Characteristics," *Tamkang Journal of Science and Engineering*, Vol. 12, pp. 271–278 (2009).

[30] Goldberg, D. E., *Genetic Algorithm in Search*, Optimization and Machine Learning. Addison Wesley (1989).

[31] Johnson, J. M. and Rahmat-Samii, Y., "Genetic Algorithms in Engineering Electromagnetics," *IEEE Antennas and Propagation Magazine*, Vol. 39, pp. 7–21, (1997).

Manuscript Received: Mar. 11, 2011
Accepted: Jun. 28, 2011